Linking in-situ information to global and planetary scale processes–

Donna Blackman
Scripps Institution of Oceanography

Framework

- Basic setting- several factors relevant to mantle dynamics
- Historical seismic basis for inference that rock deformation below Moho can be tied to mantle flow
- Linked models of microstructural deformation and mantle flow
  - spreading center mantle flow patterns
  - response(s) of multi-grain mantle rock to applied stress
  - observed grain orientation distributions & numerical predictions
  - high gradient region in uppermost mantle
- Impacts of melt in the uppermost mantle
  - anisotropic signatures
  - dike evidence for paleo-flow stresses/directions
  - re-fertilization events- impacts on evolution of deformation

Mantle Upwelling and Partial Melting

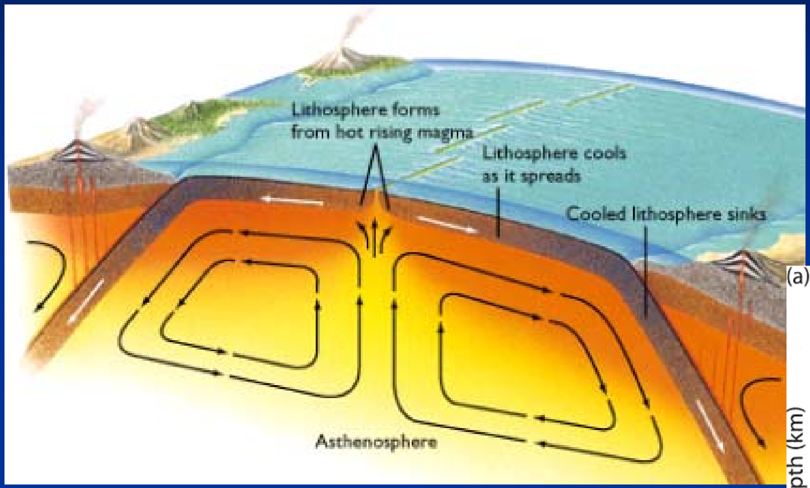

Plate-driven mantle flow

Formation of magma via partial melting during upwelling

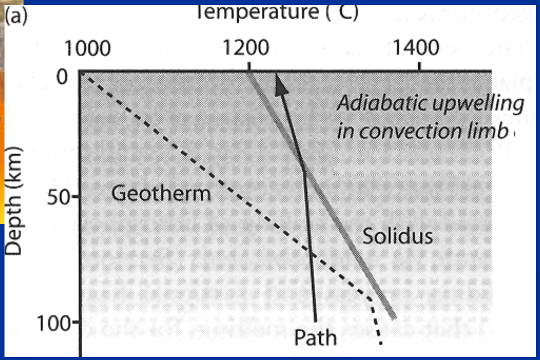

As melting proceeds, melt films connect and melt can flow in small channels

Density of melt is lower than density of residual mantle so it slowly rises

Eventually melt collects in magma chamber, cools or erupts to form crust

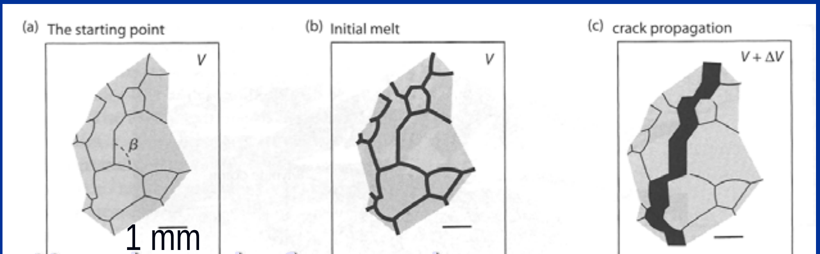

Mantle melt forms along interstices/boundaries of mineral grains

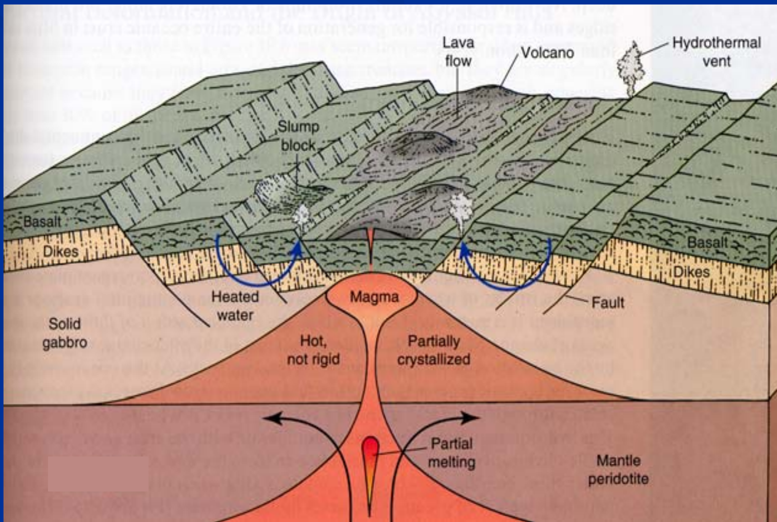

Mantle Upwelling and Partial Melting

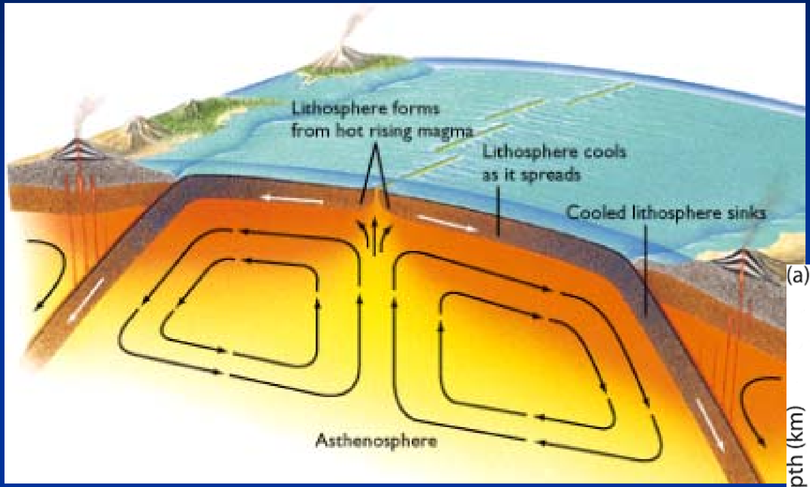

Plate-driven mantle flow

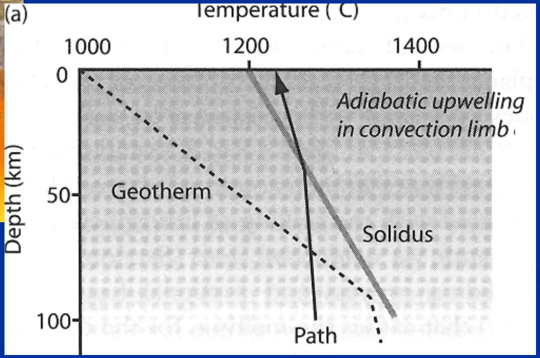

Formation of magma via partial melting during upwelling

As melting proceeds, melt films connect and melt can flow in small channels

Density of melt is lower than density of residual mantle so it slowly rises

Eventually melt collects in magma chamber, cools or erupts to form crust

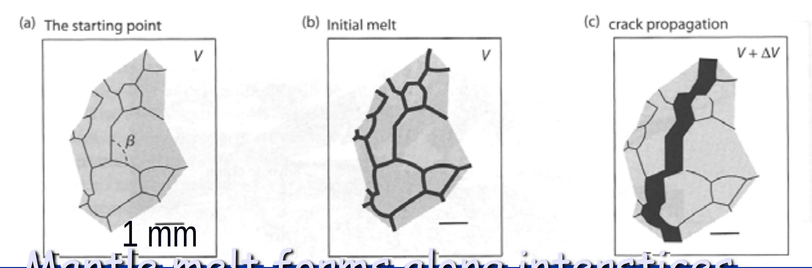

Mantle melt forms along interstices of mineral grains

I will focus on mantle part of system, (ignore) crust as rigid upper layer

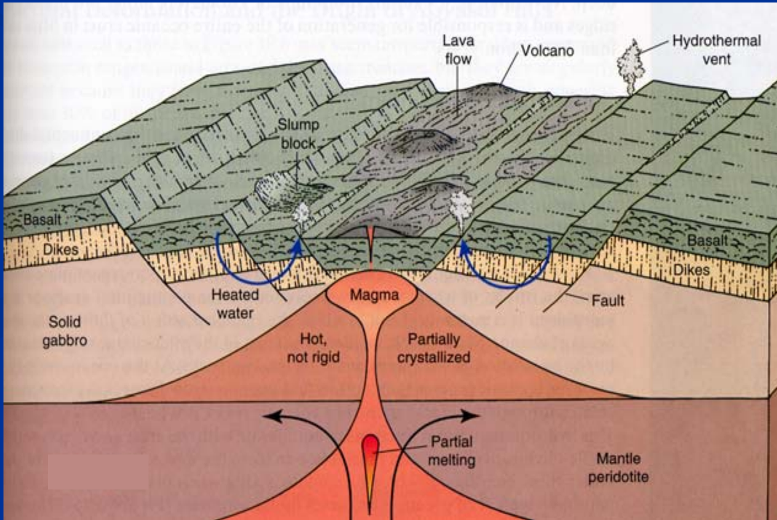

Seismic Properties of Upper Oceanic Mantle

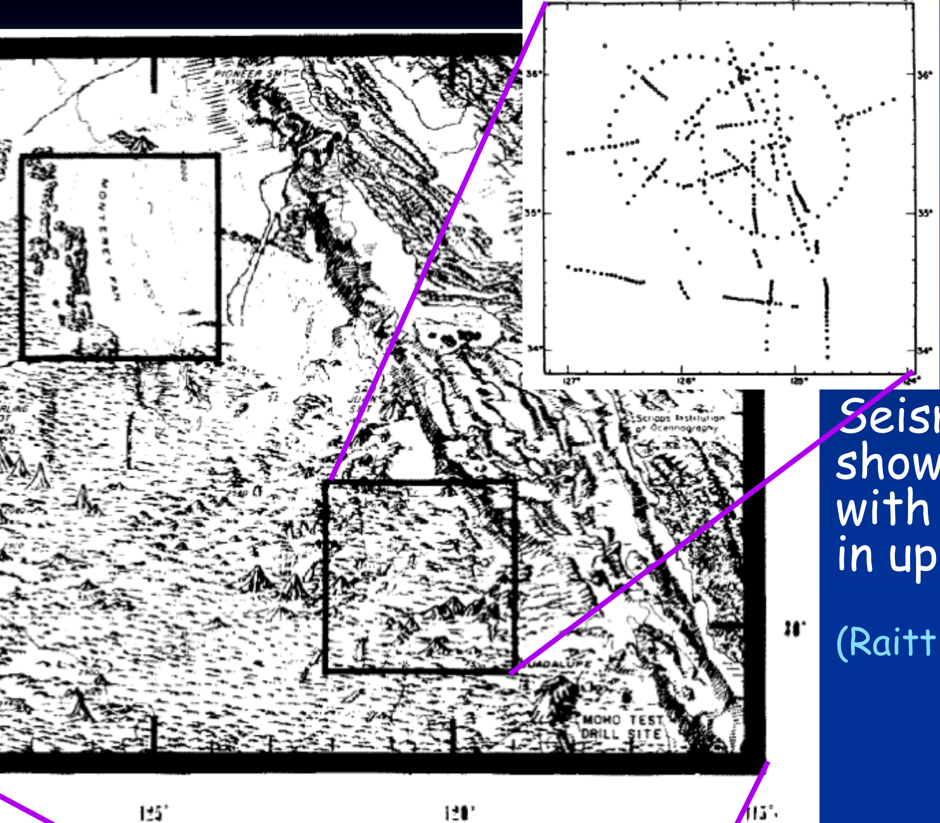

Seismic refraction shows velocity varies with P-wave direction in uppermost mantle

(Raitt et al., 1971)

Surface wave analysis shows S-wave velocity anisotropy throughout upper mantle

(Nishimura & Forsyth, 1989)

Fast P-wave in spreading direction

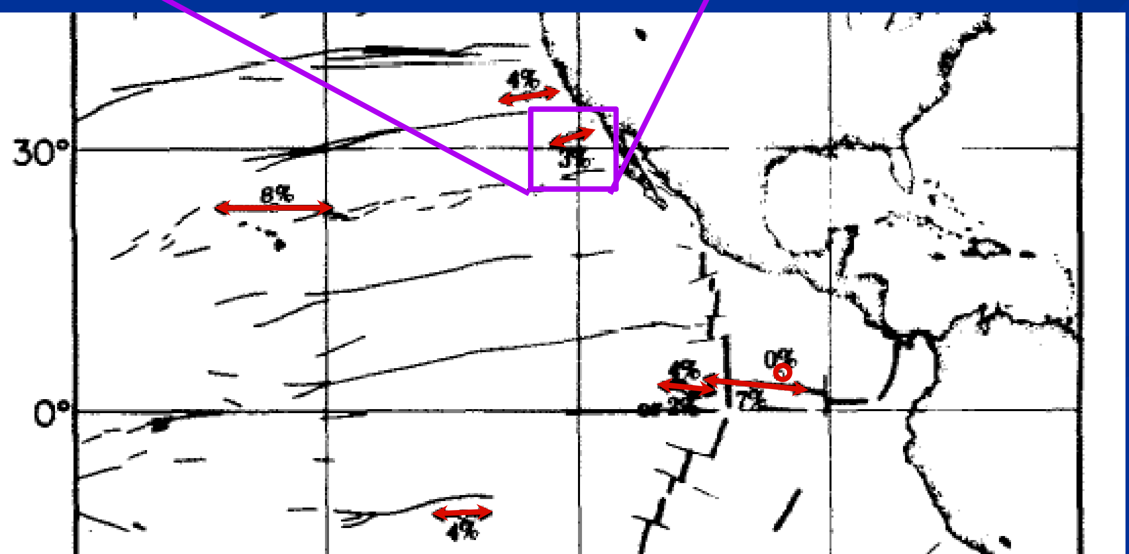

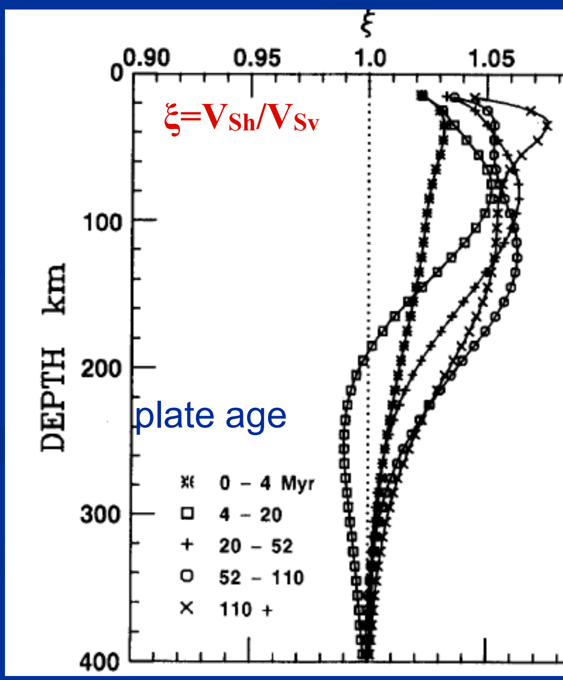

Plate-driven Mantle Flow

numerical models

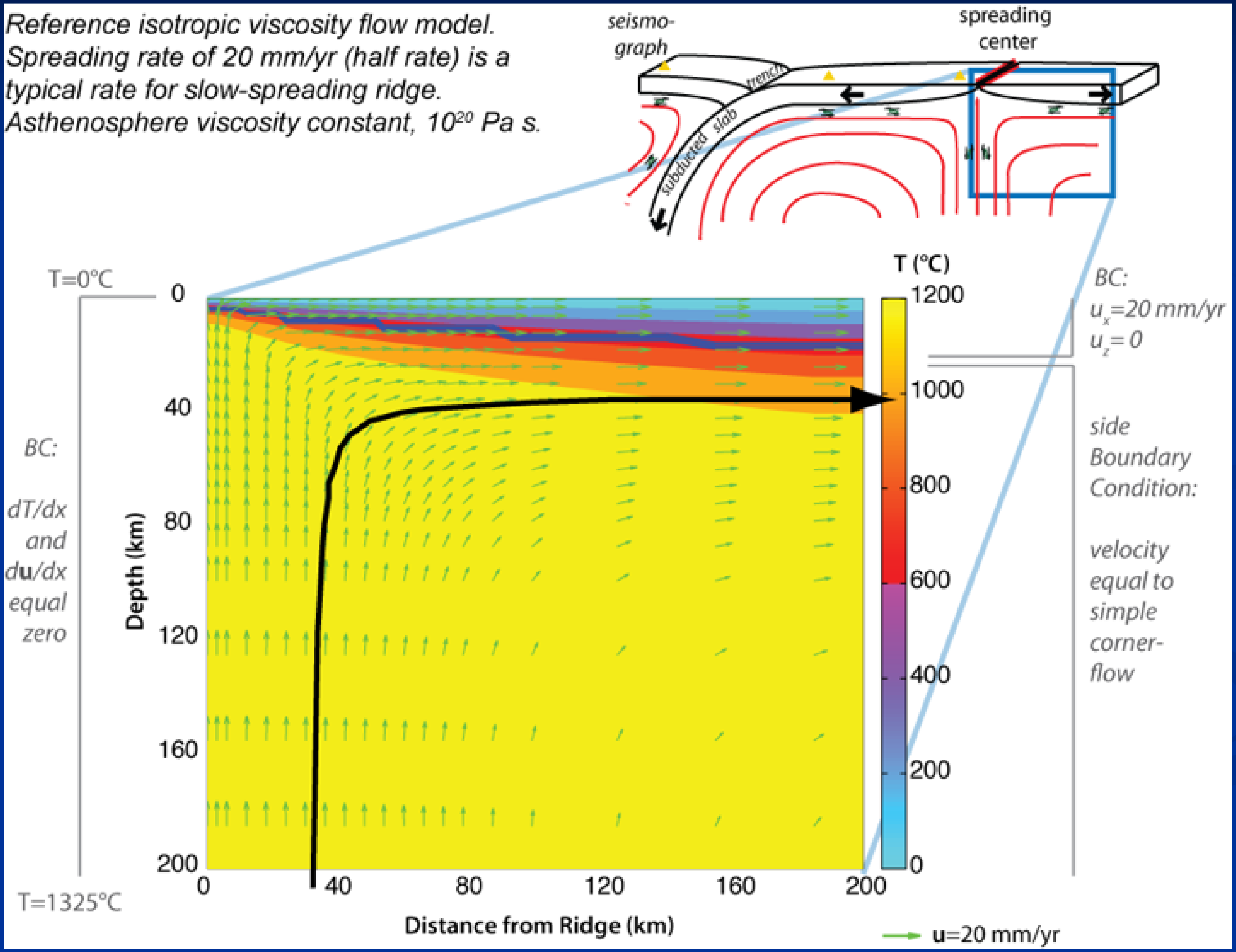

Plate-driven Mantle Flow: melt production

2-D Finite Element flow model coupled to Finite Difference temperature calculation

(Jha et al., 1994)

rigid lithosphere (<700°C)
depletion buoyancy
melt retention buoyancy

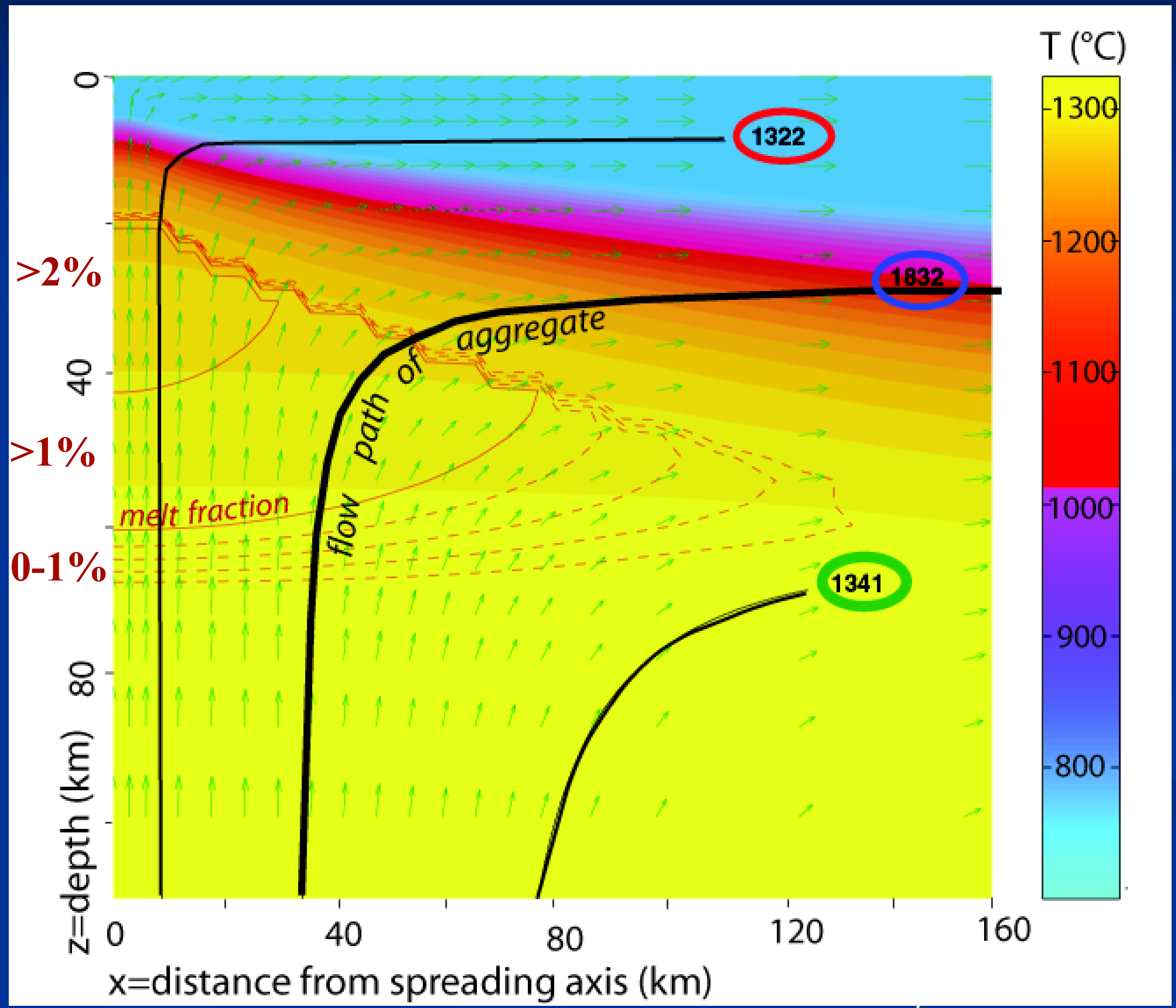

Plate-driven Mantle Flow: melt production

value assumed for (constant) asthenosphere viscosity μ, determines whether melt buoyancy forces can compete with viscous forces within flow

lower μ can result in buoyancy-enhanced upwelling, more melting

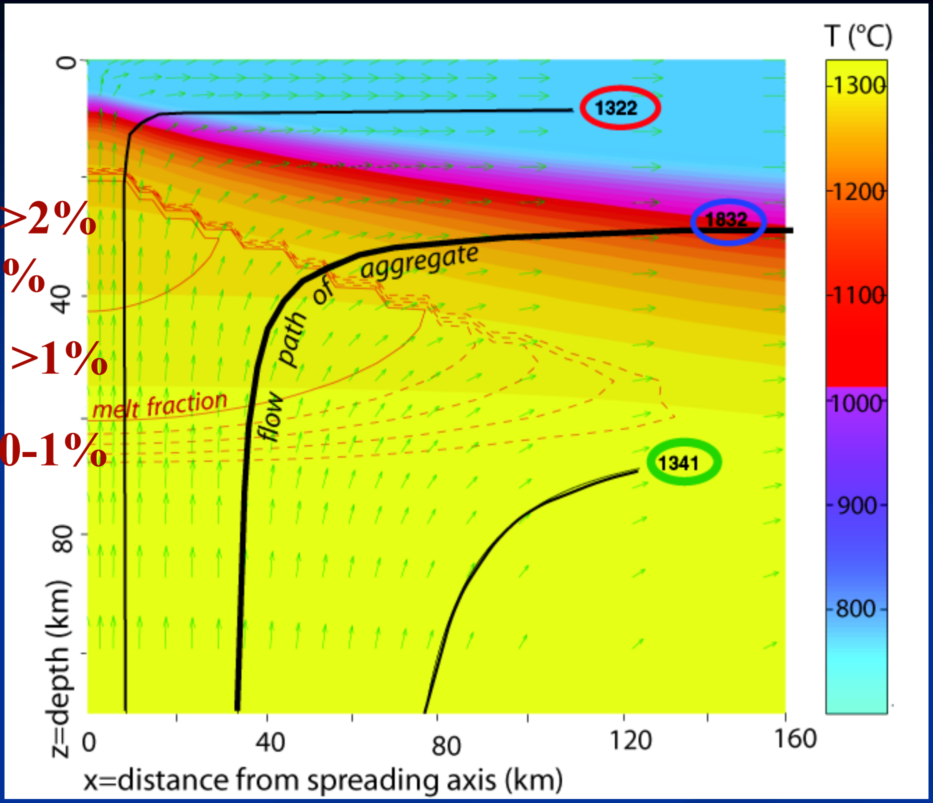

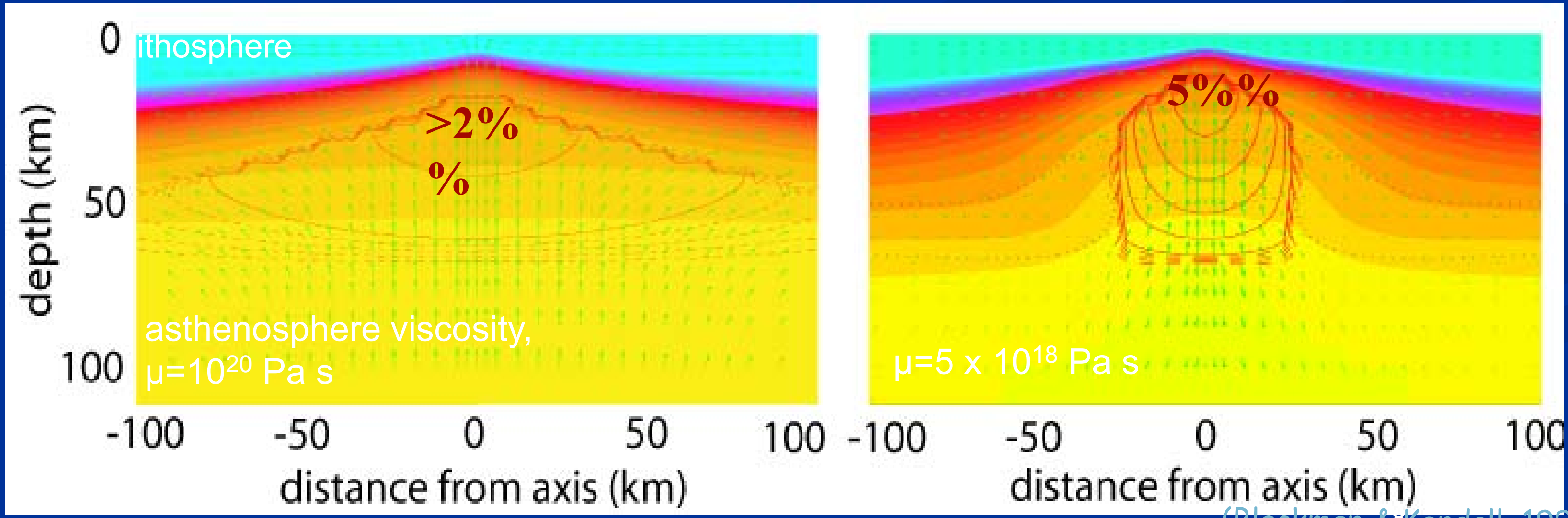

(Blackman & Kendall, 1997)

Plate-driven Mantle Flow:

parcel of mantle peridotite (polycrystal aggregate of olivine + pyroxene) encounters varying macroscopic strain rate as it transits the upwelling, corner, and sub-plate region

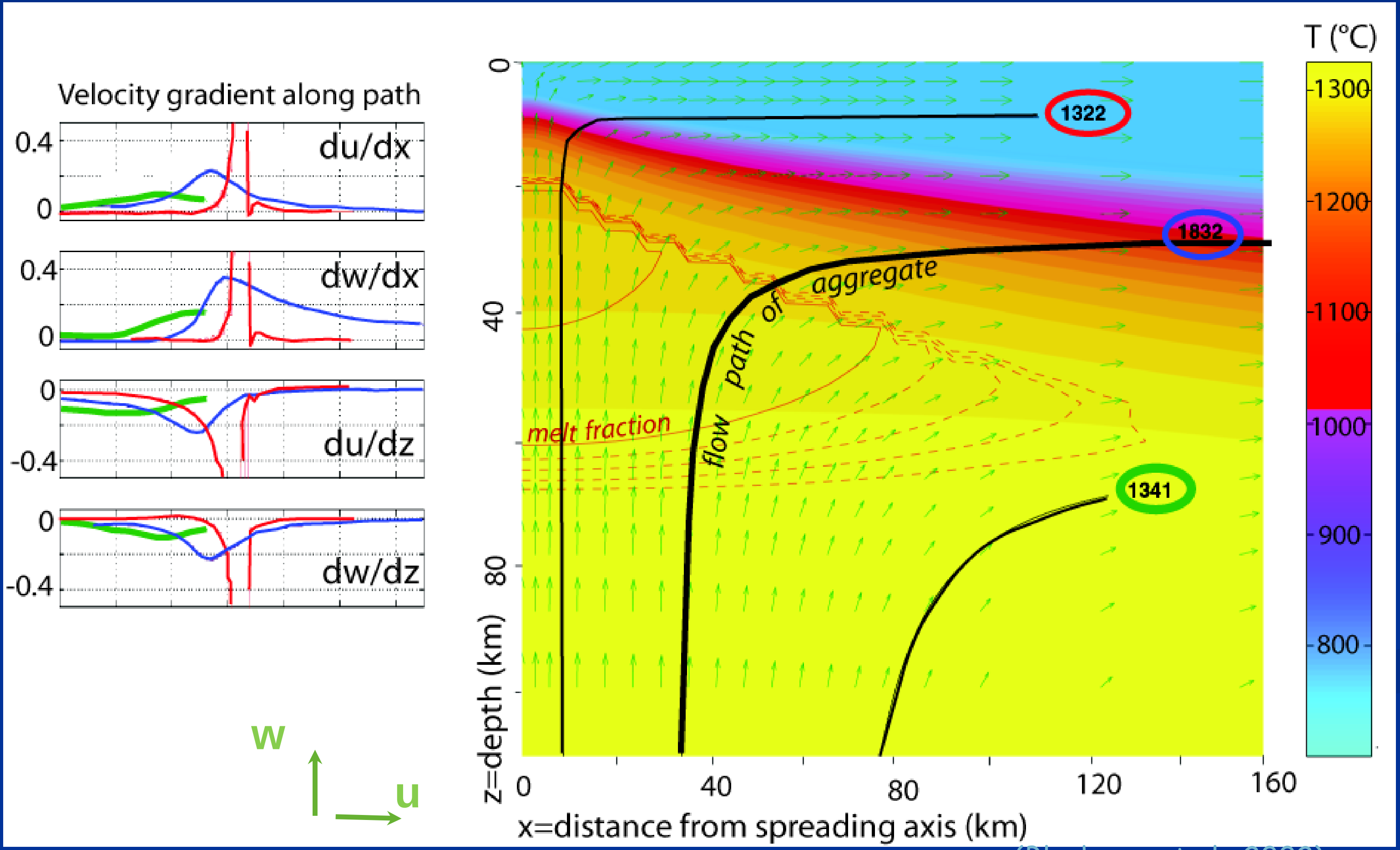

(Blackman et al., 2002)

Plastic Deformation of Mantle Minerals

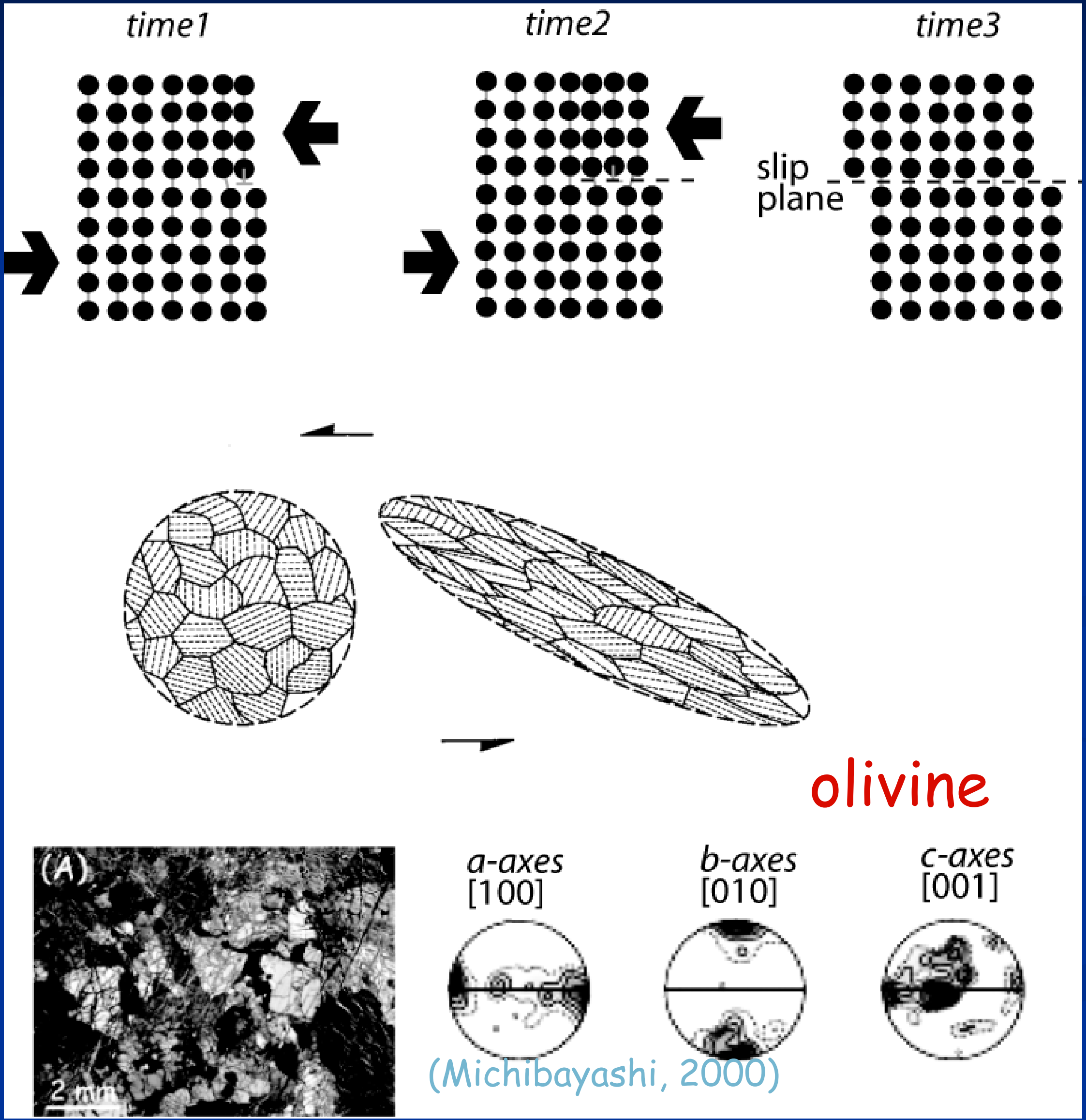

<u>Single grain</u> dislocation moves along slip plane in response to applied shear stress

<u>Aggregate of grains</u> deforms via plastic deformation of favorably oriented grains

<u>Crystal Preferred Orientations (CPO)</u> in peridotite from mantle section of Oman ophiolite

Pole figures represent CPO

Plastic Deformation of Mantle Minerals

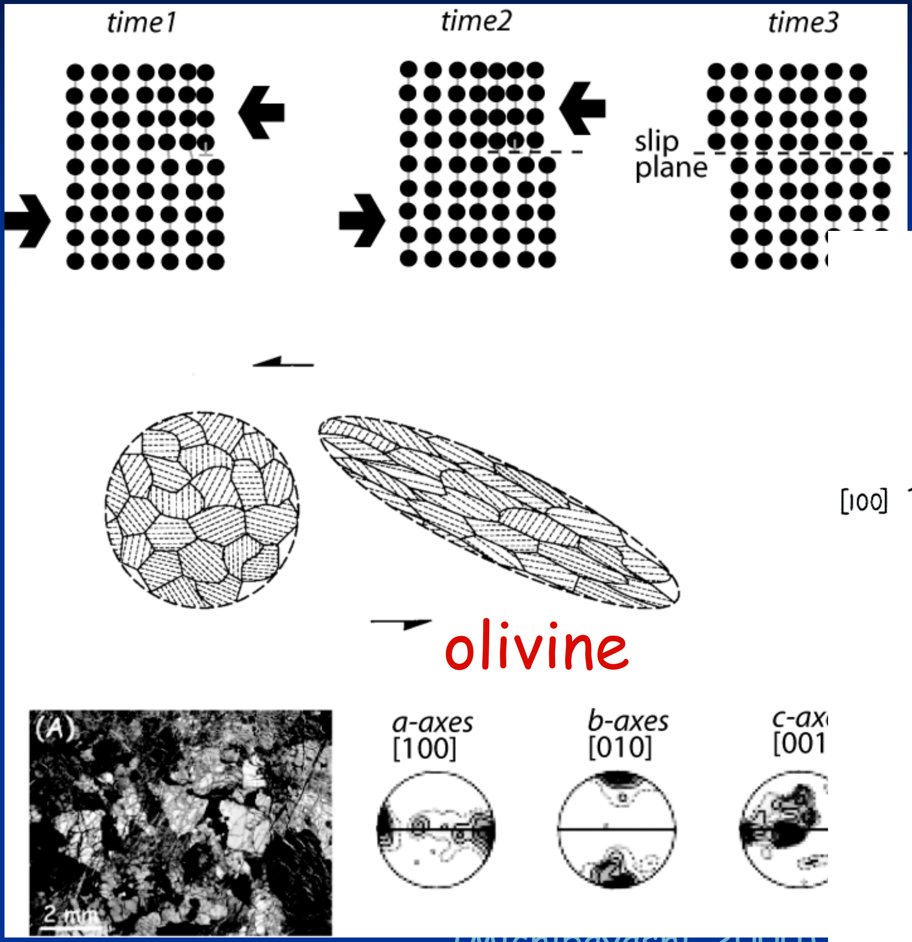

(Michibayashi, 2000)

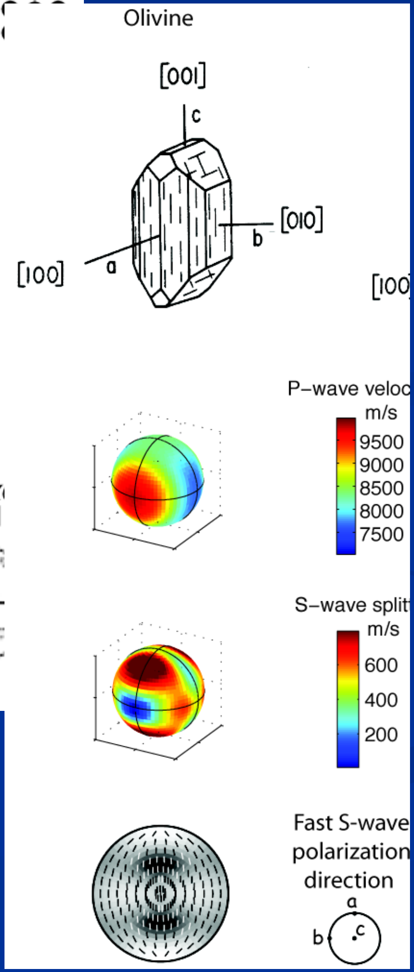

<u>Single grain</u> dislocation moves along slip plane in response to applied shear stress

<u>Aggregate of grains</u> deforms via plastic deformation of favorably oriented grains

<u>Crystal Preferred Orientations (CPO)</u> in peridotite from mantle section of Oman ophiolite

Pole figures represent CPO

Recrystallization

Laboratory experiments document behavior for shear stress
(Zhang & Karato, 1995; Zhang et al., 2000)

Initial olivine aggregate

Deformed at T=1200°C, ε=1.1

Grayshade indicates grain orientation

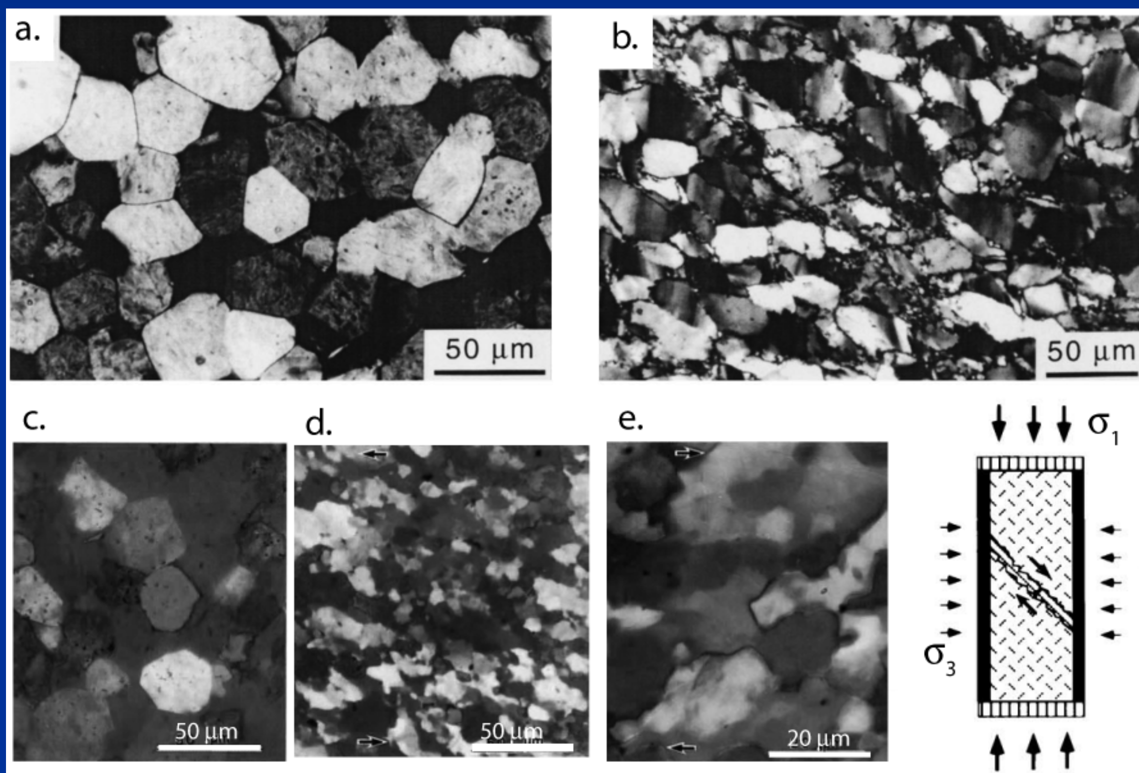

Initial

T=1300°C, ε=1.5

Subgrain rotation

Recrystallization can influence relationship between CPO and shear direction

Details of processes still being quantified-

balance of nucleation vs. grain growth

dependence on strain, stress, water content (Karato, 2008)

Numerical Simulations Of Texture Development

Assume slip system activity for each grain type (olivine, enstatite?)

Subject aggregate to strain-rate field

Compute deformation based on grain orientation and (for VPSC) influence of surrounding matrix

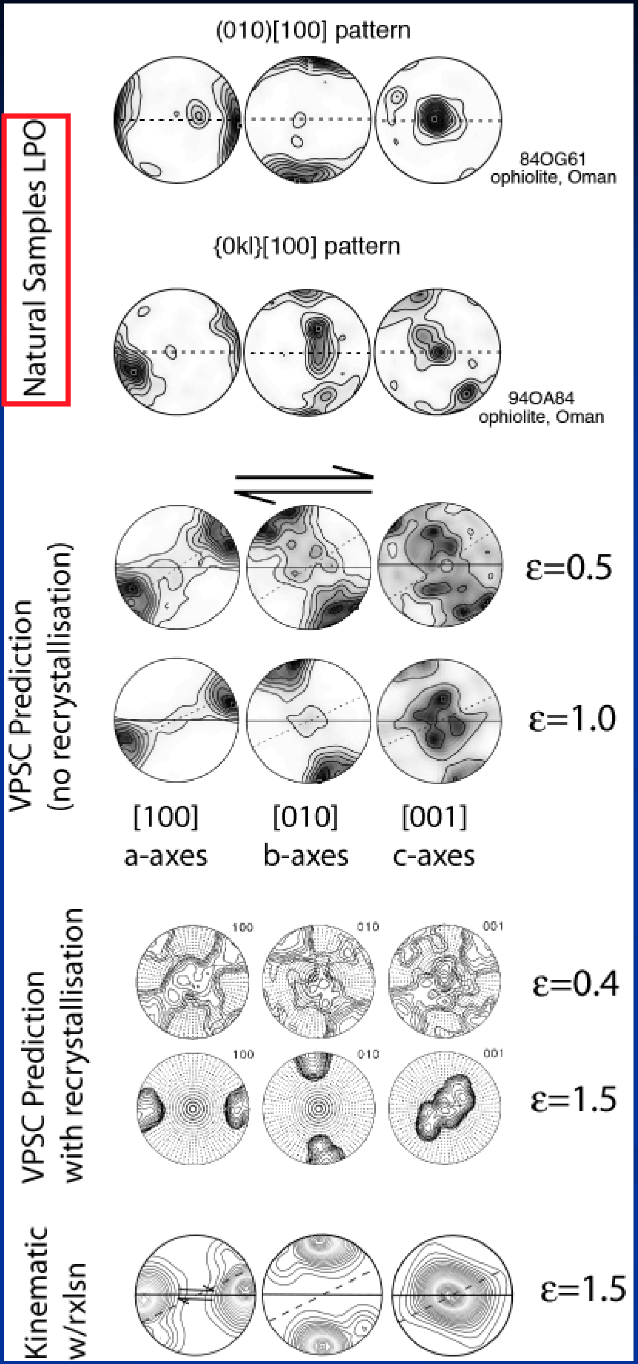

Olivine CPO

Comparison between progressive simple-shear predictions and natural samples (Ben Ismail & Mainprice, 1998)

Viscoplastic Self-Consistent (VPSC) method (Wenk et al., 1991)

VPSC with nucleation & grain growth (Wenk & Tome, 1999)

Kinematic theory (Kaminsky & Ribe, 2001; 2004)

Prediction- steady shear beneath oceanic plate

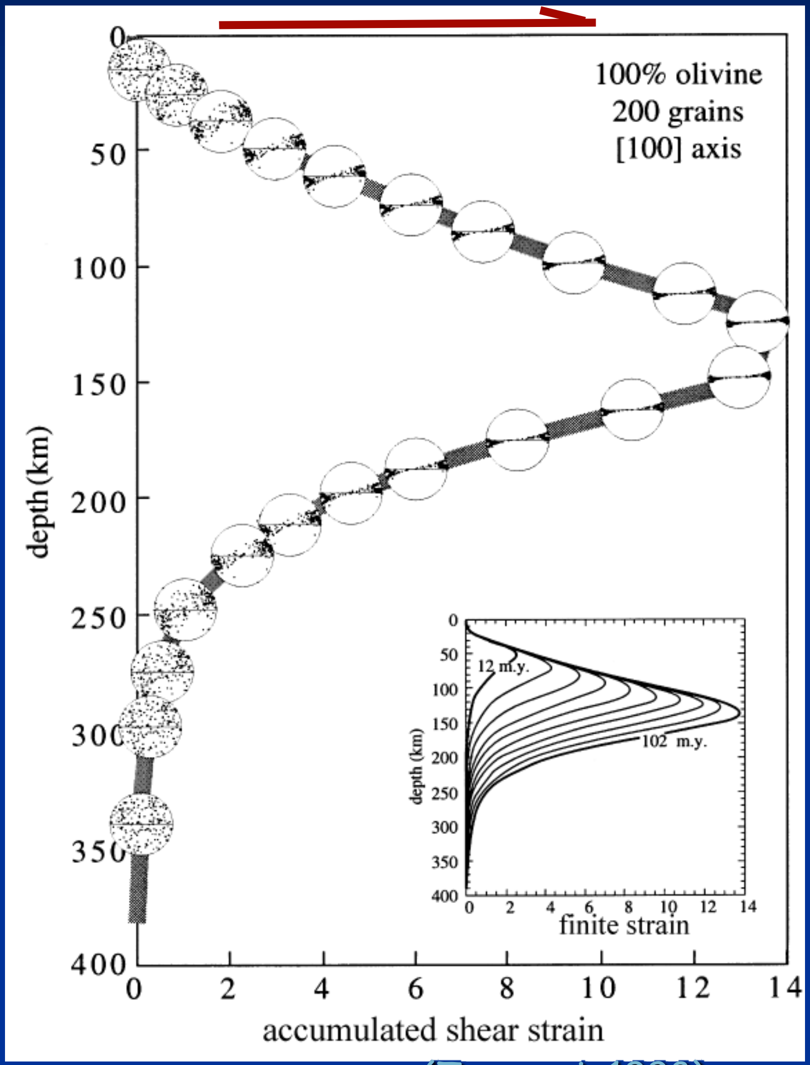

(Tommasi, 1998)

2-D FEM

VPSC (no recrystal-lization) model of texture development

Zone of strong CPO thickens and deepens with plate age

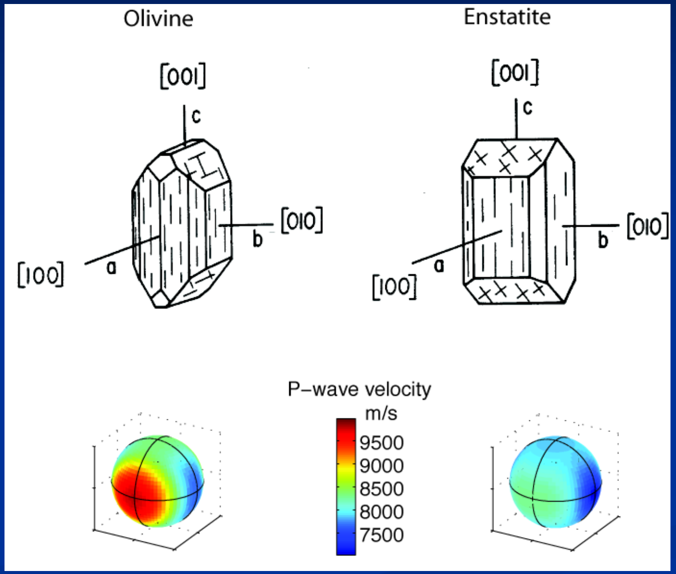

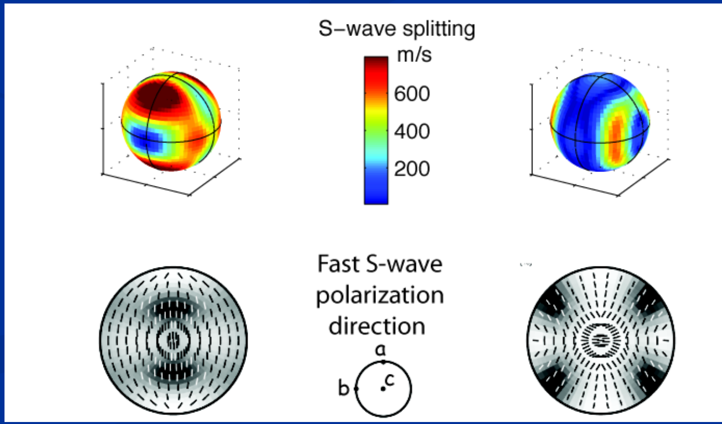

Compute effective elastic properties of aggregate by projecting single-crystal elastic constants

Shear Wave Splitting determined with the MELT OBS array

(Wolfe et al., Science 1998)

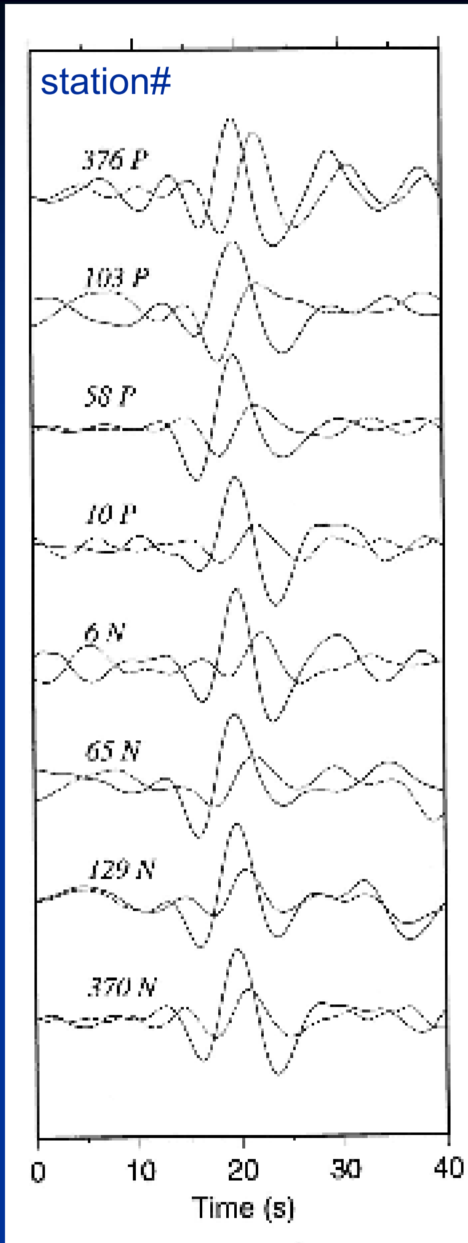

Seismograms show delay between slow and fast S-wave

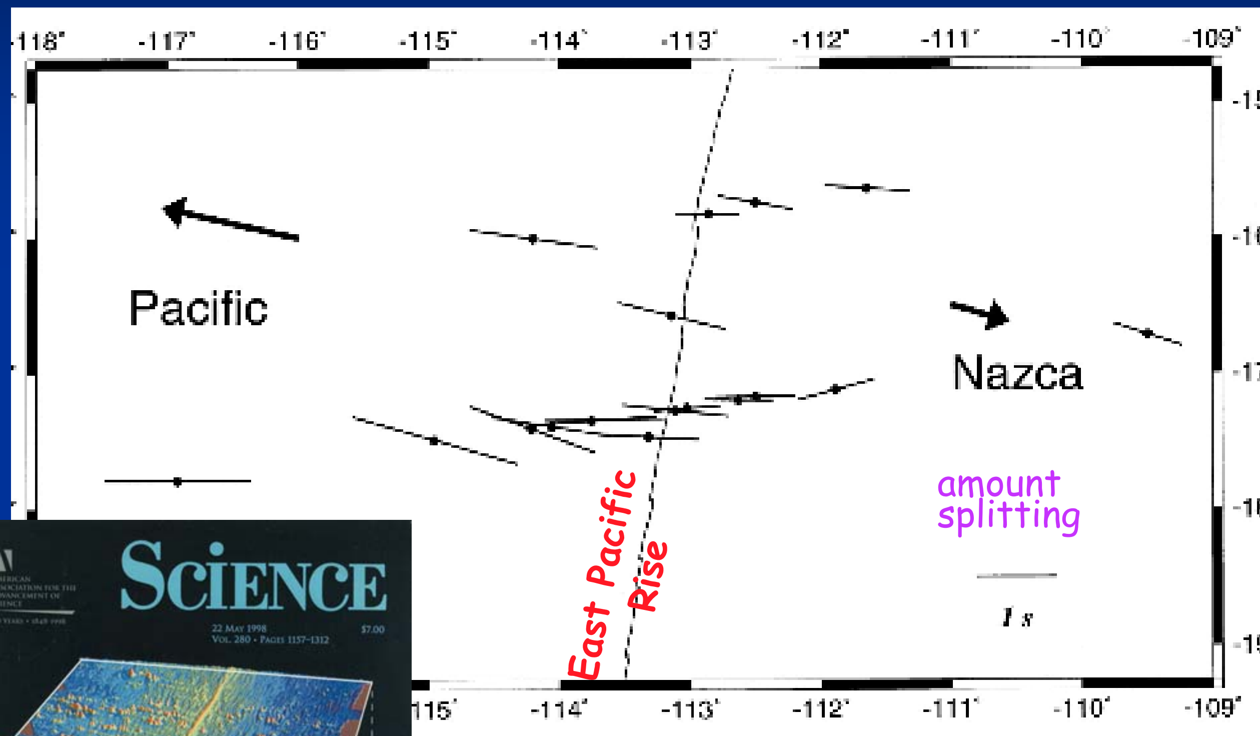

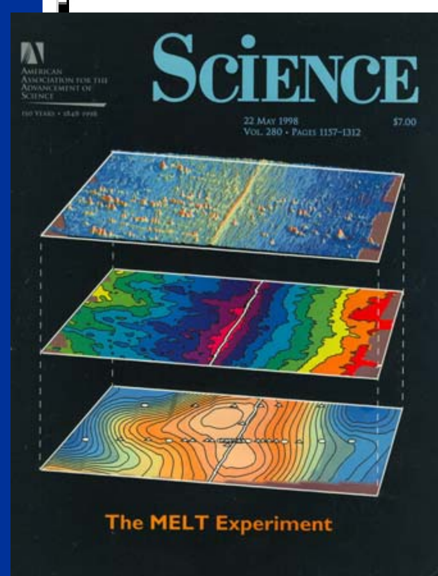

- Collaborative project of RIDGE program
- First ~year-long Ocean Bottom Seismometer experiment
- EPR migrates over deep mantle

Reference EPR 17°S Flow Model

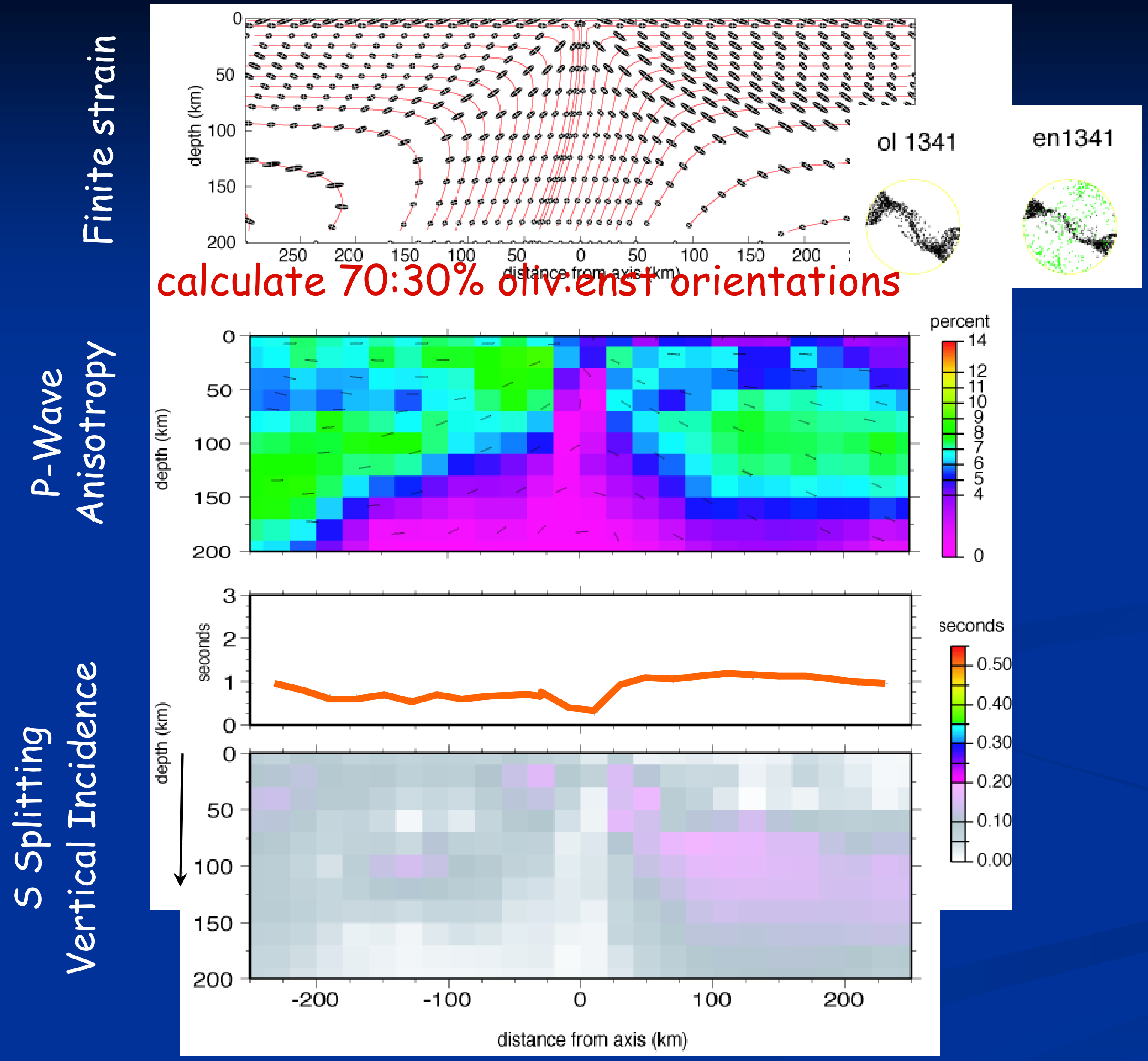

Spreading axis migrates west at 32 mm/yr

Constant asthenospheric viscosity, below rigid lithosphere

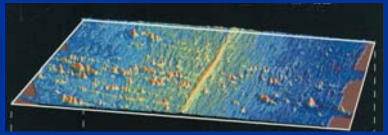

EPR 17°S model

T-Pressure dependent viscosity, no flow thru 660

Conder et al. 2002

Textural anisotropy model

Blackman & Kendall, 2002

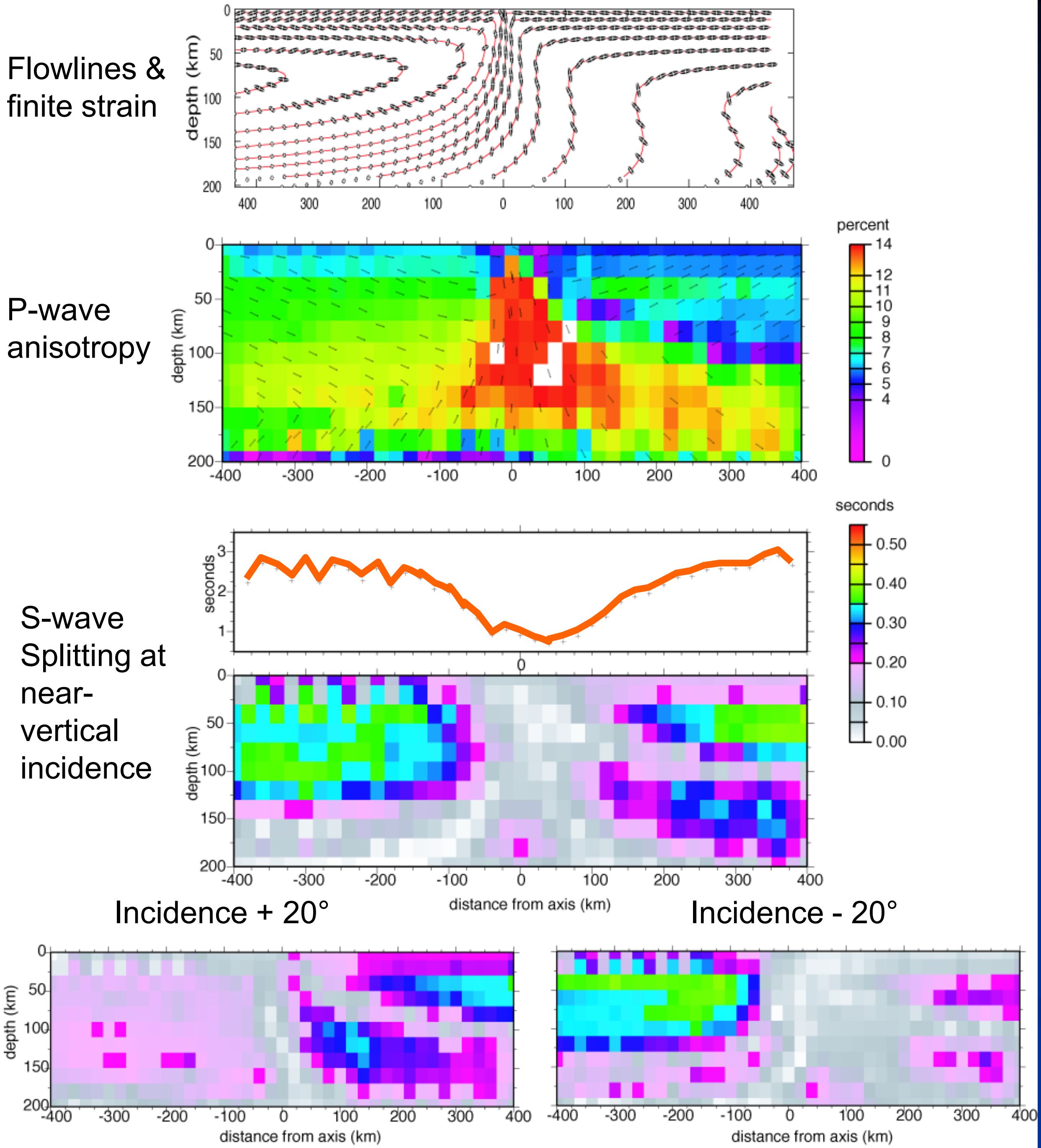

Predictions for this model do not match MELT splitting results although predicted temperature & melting are consistent with P-wave delay pattern

EPR 17°S model

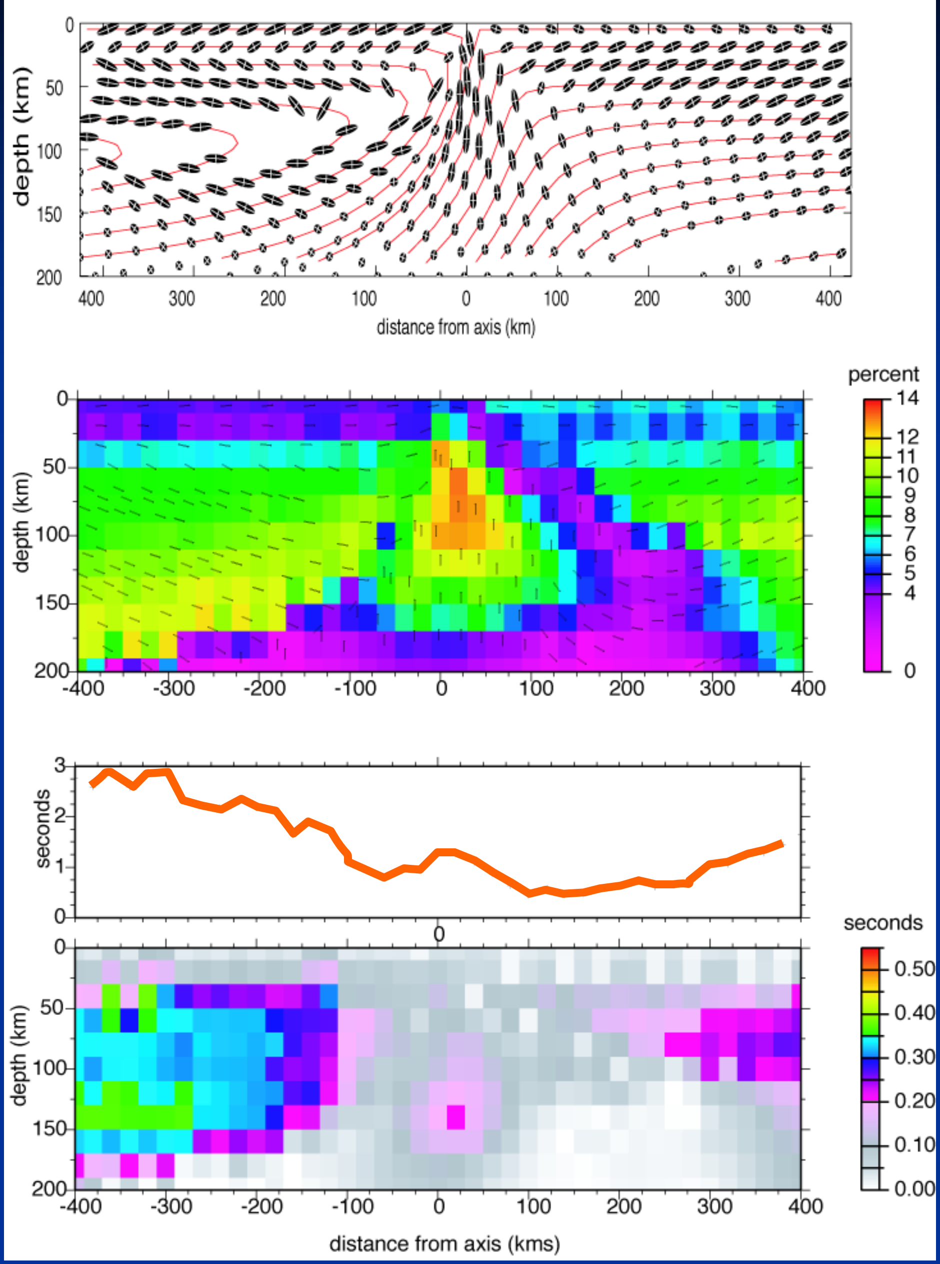

Temperature Anomaly associated with Pacific Superswell influences flow (Toomey et al., 2002)

Predictions for seismic anisotropy & P-wave heterogeneity match MELT data better than the other models tested

>> ability to distinguish between flow models

Shear Wave Anisotropy-

MELT + GLIMPSE results combined

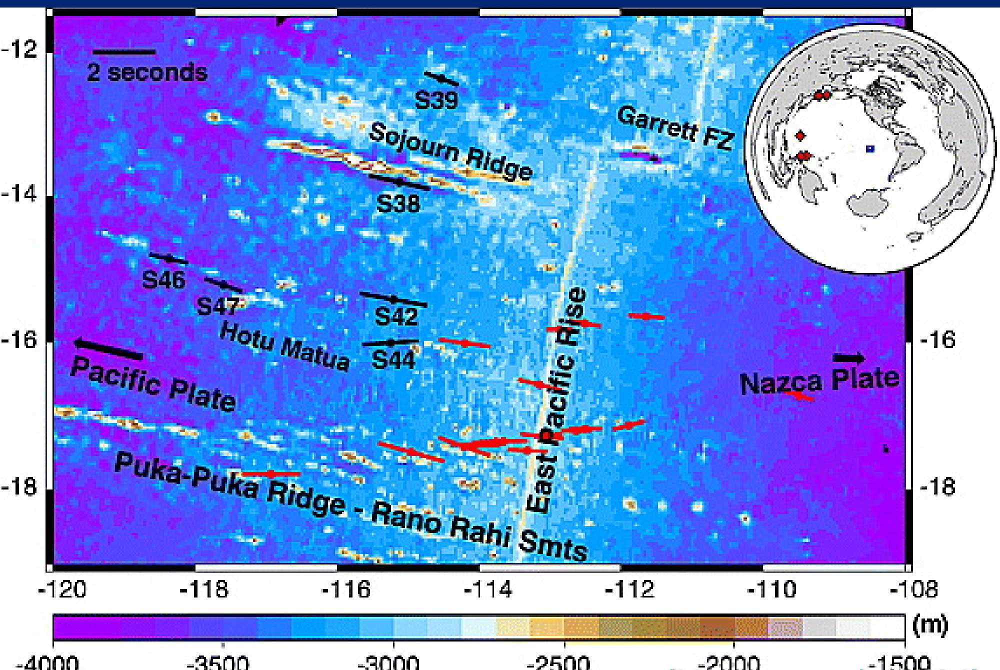

(Harmon et al., 2004)

S-wave splitting does not continue to increase with plate age on W flank onset of small-scale convection beneath plate??

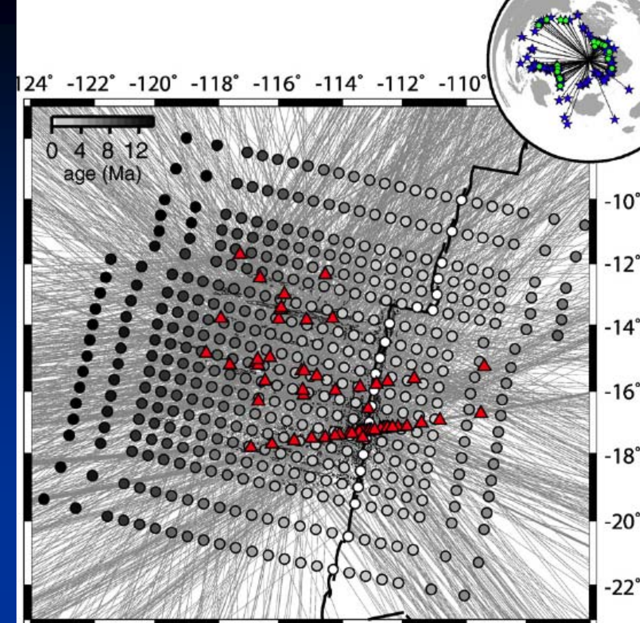

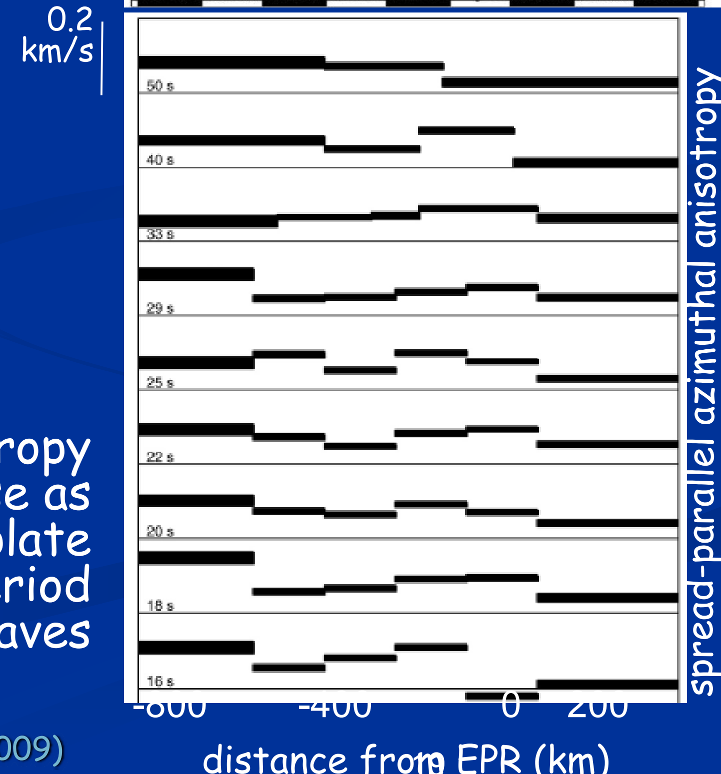

azimuthal anisotropy does not increase as simple function of plate age for short period Rayleigh waves

(Harmon et al., 2009)

Factors other than flow-induced deformation

feedbacks between microstructure, rheology, & flow pattern
melt distribution(s)
temperature (asthenosphere vs. lithospheric mantle)
grain size and water content (small but non-zero)
mode of deformation affects LPO (development or destruction)
macroscopic viscosity affected

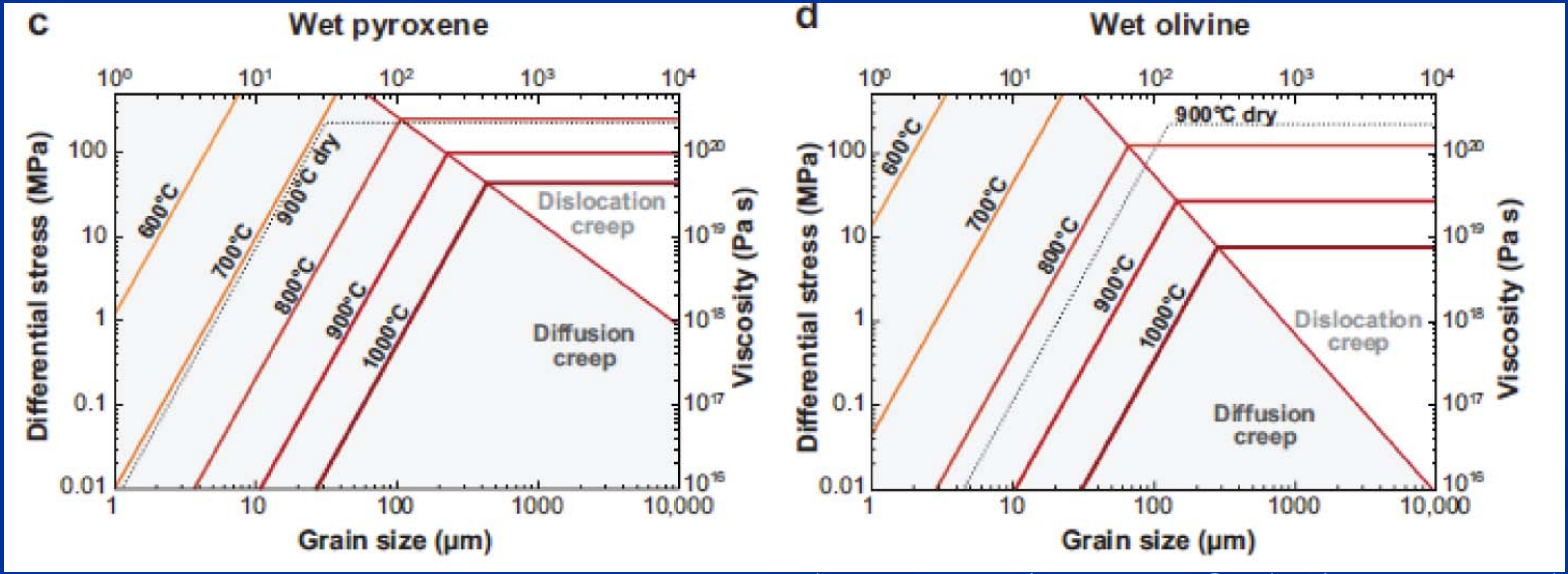

(Bürgmann et al., Ann. Rev. Earth Planet. Sci, 2008)

Aligned Melt in the Mantle- observation

Seismometer array deployed at Ethiopian Rift for ~2 yrs detected subaxial velocity anomalies and SKS-wave anisotropy (Kendall et al., 2005)

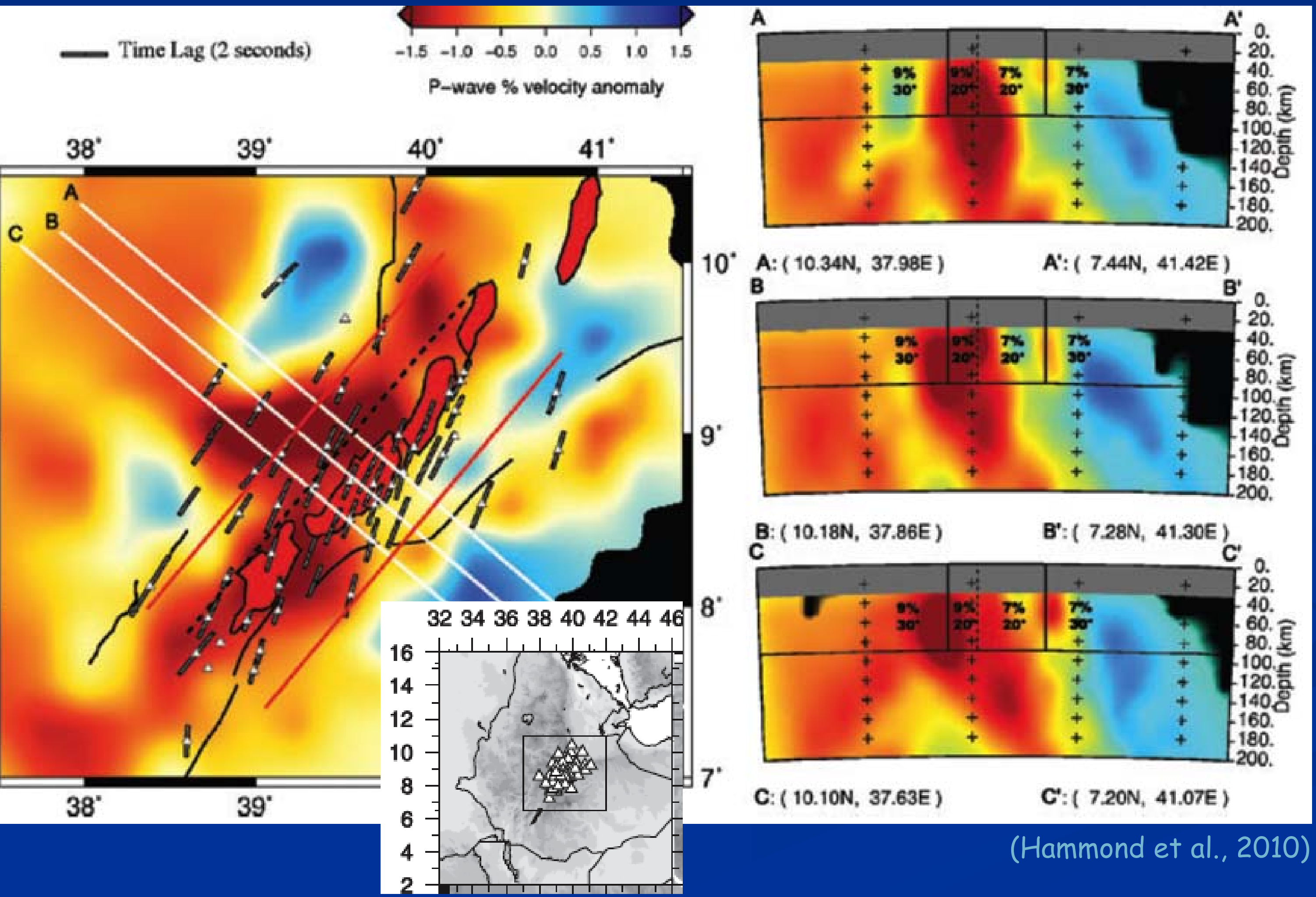

alignment of fast S-wave polarization in direction of rift axis and pattern of delays wrt axis suggests vertically-aligned melt channels

(Hammond et al., 2010)

Aligned Melt in the Mantle-numerical model

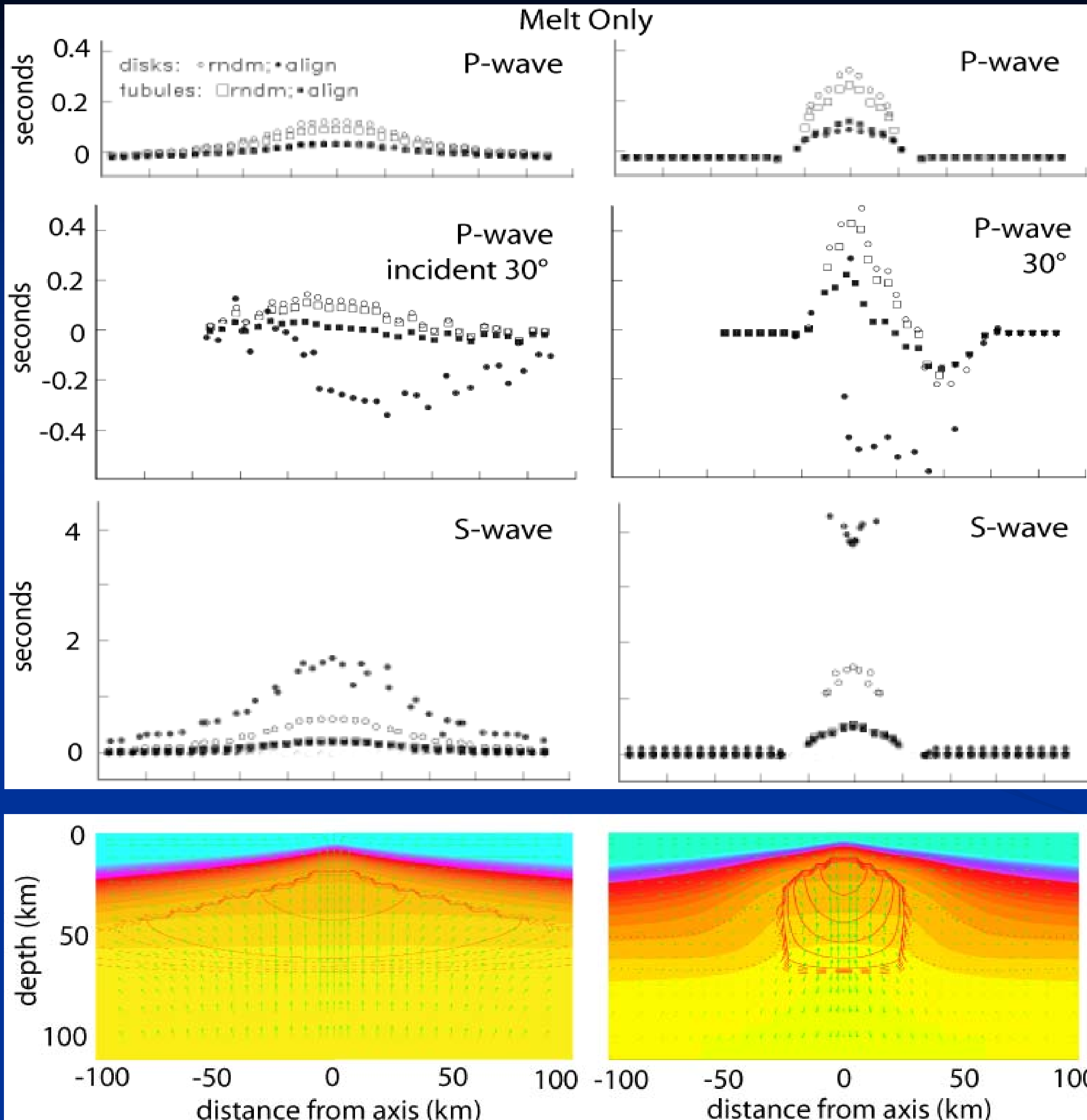

(Blackman & Kendall, 1997)

Tubules simulate melt at grain intersection

Disks simulate melt along grain boundaries

Theory after Hudson (1980) and Tandon & Weng (1984)

Aligned disks model assumes vertical alignment

what signal if this melt drains (up) or if it crystallizes in place?

Aligned Melt in the Mantle-field evidence

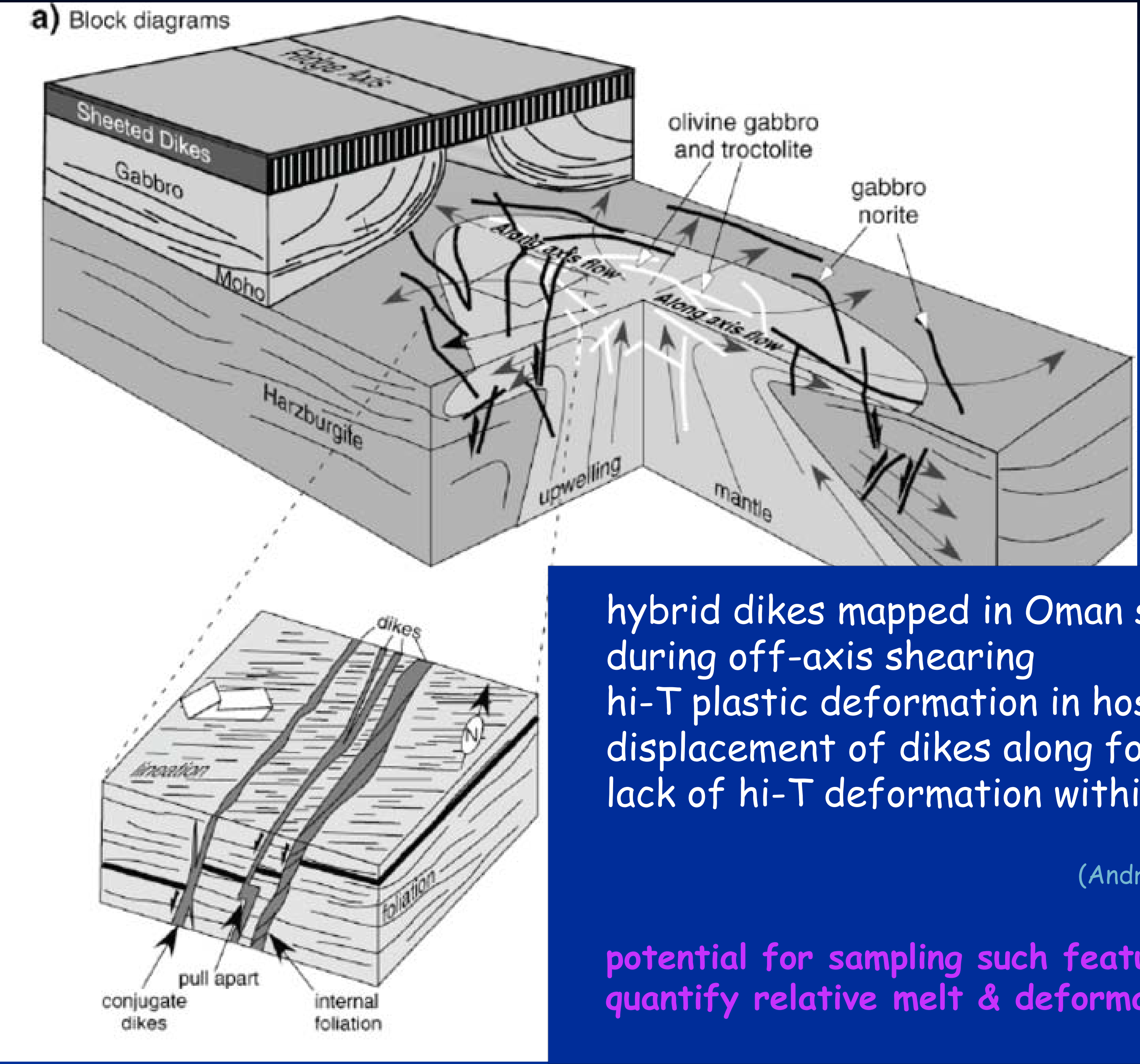

hybrid dikes mapped in Oman suggest injection during off-axis shearing
hi-T plastic deformation in host peridotite
displacement of dikes along foliation
lack of hi-T deformation within dike

(Andronicos et al., 2009)

potential for sampling such features in a MoHole, quantify relative melt & deformation stresses

Infiltration by Later Melt

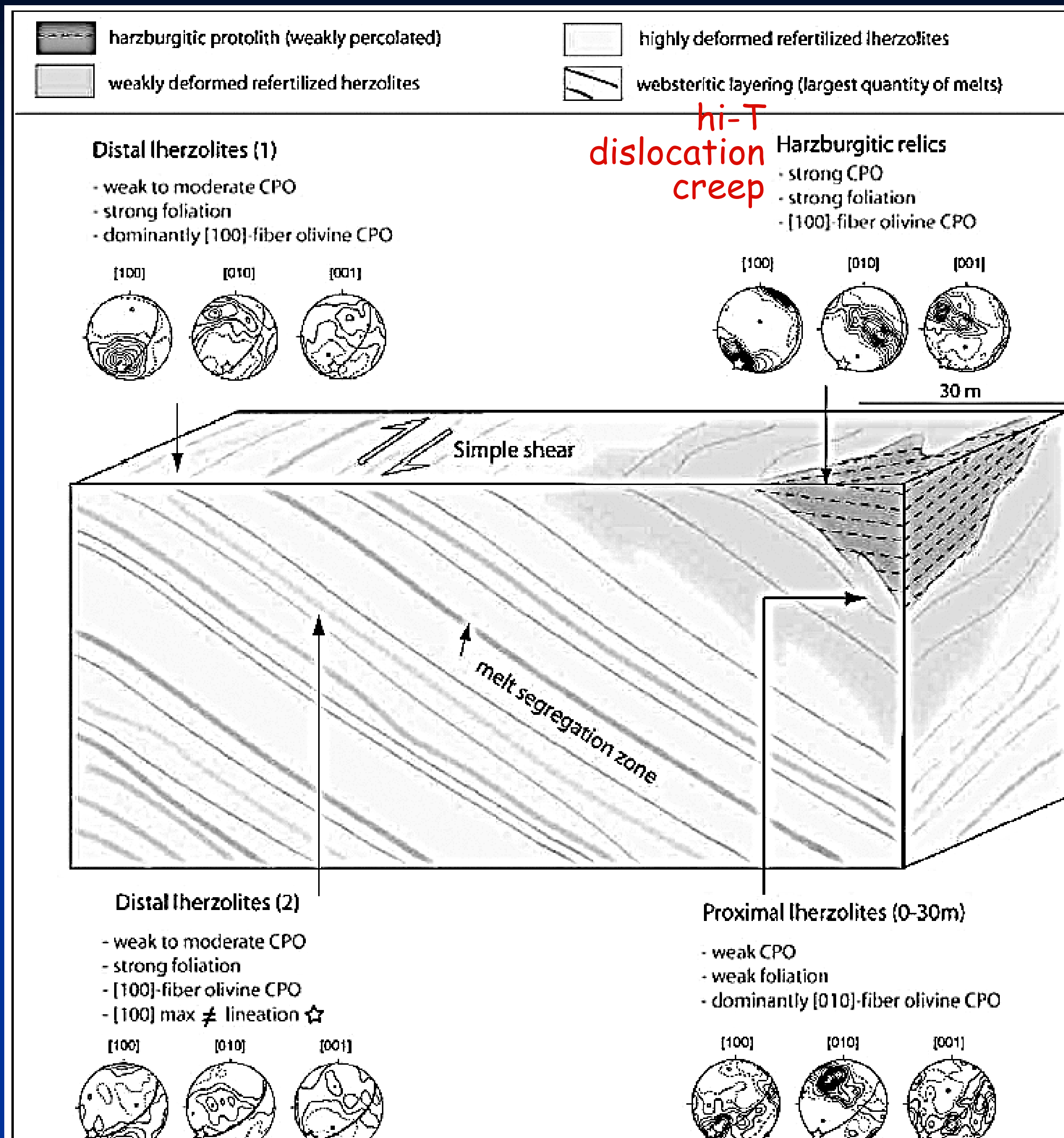

Field studies in Lherz Massif, Pyrenees, indicate strong feedback between melt percolation & deformation

deformation localized in melt-permeated zone, away from host harzburgite

evolution of macroscopic structures & CPE >> variations in finite strain and in melt fraction present during deformation

(LeRoux et al., 2008; other recent studies A Tommasi & coworkers)

massif emplaced ~110 Ma; refertilization by later basalt melt

Implications for MoHole Studies

- MoHole investigations within mantle section would document structure and ground truth physical properties
  - crystal-plastic deformation/annealing, in-situ (paleo)melt distributions, extents of melt-host reaction & equilibrium, extents & nature of any alteration
    - new magneto-telluric results consistent w/aligned serpentinite zones (S Constable & coworkers)

Challenges...

- uppermost mantle likely to be complex
  - melt (subaxial & off-axis), deformation gradients
  - some structures may be quite localized and regions in between may show little deformation/melt interaction/alteration (Achenbach et al., ODP Leg 209 results)
- plate spreading shear, possible change in plate motion (?) could overprint primary structures

Extending Mantle Insights for MoHole

- borehole logging- seismic, resistivity, imaging
- borehole seismometer(s) in mantle section
  - active-source experiment to assess azimuthal variation in velocity
  - passive (earthquake) experiment for deeper info: S-wave splitting, azimuthal dependence for shallow incidence?

- Walk-away Vertical Seismic Profiling and circular shooting line around MoHole
  - multiple seismometer stations within hole
  - OBS profiles radiating from hole
  - deep, low-frequency source (for mantle-traveling waves)
    - also opportunity to study lower crustal, uppermost mantle reflectivity in detail